The Astrophysical Journal, 529:L99–L102, 2000 February 1

RECENT CHANGES IN THE NEAR-INFRARED STRUCTURE OF η CARINAE[1]

Nathan Smith and Robert D. Gehrz
Department of Astronomy, University of Minnesota, 116 Church Street, SE, Minneapolis, MN 55455;
nathans@astro.umn.edu, gehrz@astro.umn.edu
Received 1999 September 23; accepted 1999 December 6; published 1999 December 30

ABSTRACT

Near-infrared imaging at two phases in the 5 yr spectroscopic cycle of η Carinae reveals changes in the spatial structure of the inner core that may be related to recently reported near-infrared photometric variability. The central source changed from a pointlike object to a more extended, bipolar or shell structure. This behavior is reminiscent of changes observed in the radio continuum. NICMOS images show a toroidal distribution of dust and gas around the central star and confirm the morphology of several other structures observed in ground-based images of the Homunculus. The morphological variations appear to be confined to the central core of the nebula.

Subject headings: circumstellar matter — stars: individual (η Carinae)

1. INTRODUCTION

The central engine that powers the bipolar "Homunculus" nebula around η Carinae has a luminosity of $10^{6.7}$ $L_\odot$ and an effective temperature of 30,000 K (Davidson 1971). Details of how the radiated energy is processed as it escapes through the more than 2 $M_\odot$ of gas and dust that surrounds and partially obscures the star remain elusive. Deductions of the structure in the core of the nebula using optical observations is complicated by the considerable extinction from circumstellar dust. This problem can be mitigated using near-infrared (IR) observations that penetrate the dust screen.

The near-IR spectrum of η Car through a large aperture contains a wealth of emission lines from H I, He I, Fe II, and [Fe II], superposed on a continuum that rises gradually with increasing wavelength (Whitelock et al. 1983; Allen, Jones, & Hyland 1985). Imaging with narrow filters suggests that the near-IR emission lines are primarily confined to the bright core, and the bipolar lobes and equatorial ejecta of the Homunculus are seen in scattered light at near-IR wavelengths with a morphology similar to optical images (Smith, Gehrz, & Krautter 1998, hereafter SGK). Early maps of η Car at 2.2 μm show that the central core was extended and double-peaked in a direction roughly perpendicular to the major axis of the Homunculus (Mitchell et al. 1983). This is similar to the morphology of the core at longer IR wavelengths dominated by thermal emission from warm dust (Hyland et al. 1979; Hackwell, Gehrz, & Grasdalen 1986; Smith et al. 1995; SGK). Near-IR adaptive optics images by Rigaut & Gehring (1995, hereafter RG) show a "crescent-shaped" feature elongated in a direction roughly perpendicular to the major axis of the Homunculus at an intensity level of 0.15% of the central peak in the *K* band, which is interpreted as a circumstellar equatorial torus with a radius of 2800–3800 AU (the distance to η Car is ~2.3 kpc; Meaburn 1999).

The near-IR photometric variability of η Car discussed by Whitelock et al. (1994) shows a period of ~5 yr in the *JHKL* light curves, and Daminelli (1996) suggested a 5.52 yr period defined by the disappearance of high-excitation lines during a "spectroscopic event." The cause of the 5 yr period and spectroscopic events remains controversial (see contributions in Morse, Humphreys, & Daminelli 1999). The near-IR structures observed by Mitchell et al. in 1980 and RG in 1991 suggest that there may be some variability in the core region, but it is unclear how it relates to the ~5 yr photometric variability. The observations analyzed here yield a detailed view of the near-IR emission from the core region of η Car and provide a comparison with earlier images to reveal morphological changes in the core related to the 5 yr spectroscopic cycle.

2. OBSERVATIONS

Observations of η Car were obtained with the *Hubble Space Telescope* (*HST*), using camera 2 of the Near-Infrared Camera and Multiobject Spectrometer (NICMOS), on 1998 September 6 and entered the public archive 1 year later. We compared these observations with the 2 μm images made in 1995 May by SGK in order to search for morphological changes related to η Car's recently reported near-IR photometric and spectroscopic variability. The narrowband *HST* images were obtained from the *HST* public archive and processed using standard CALNICA and CALNICB procedures. The broadband NICMOS images that were obtained as part of the same program suffered from severe saturation. The exposures were not dithered, so bad pixels on the array had to be corrected by interpolating using adjacent pixels. Since the central core is much brighter than the surrounding nebula, the images were strongly affected by the telescope's point-spread function (PSF). A few pixels at the location of the central star were overexposed in the shortest MULTIACCUM readouts. Tiny Tim (see the *HST* Data Handbook) was used to fabricate a model of the PSF for each filter that was then normalized to the level of the PSF in the NICMOS exposures through an iterative fit to several bright points in the PSF wings and airy disks. The normalized 2.15 μm PSF had an integrated flux of 1.1×10^{-11} ergs cm^{-2} s^{-1} Å^{-1}, contributing roughly half the flux from the entire Homunculus at 2.15 μm. The overexposed pixels on the central star were replaced using the normalized Tiny Tim PSF. The fabricated PSF was used as a model PSF for 10 iterations of the standard Lucy-Richardson deconvolution task in IRAF. The results of the deconvolution show minor pixel-to-pixel artifacts caused by imperfect

[1] Based on observations made with the NASA/ESA *Hubble Space Telescope*, obtained at the Space Telescope Science Institute, which is operated by the Association of Universities for Research in Astronomy, Inc., under NASA contract NAS5-26555.

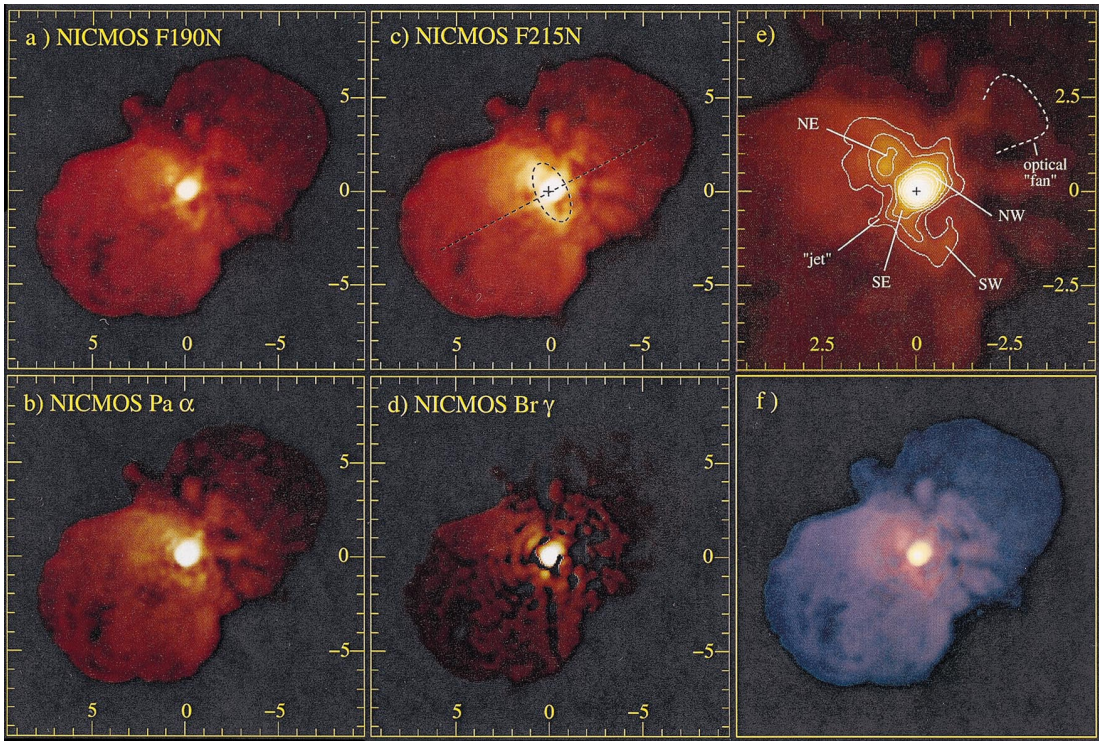

FIG. 1.—NICMOS images of η Car. The axes denote right ascension and declination offsets from the position of the central star in arcseconds. (*a*) 1.9 μm continuum (F190N filter), (*b*) continuum-subtracted Paα emission (F187N–F190N), (*c*) 2.15 μm continuum (F215N filter), and (*d*) continuum-subtracted Brγ emission (F216N–F215N). In (*a*)–(*d*), the false-color intensity scale ranges from 0 to 5×10^{-14} ergs s^{-1} cm^{-2} Å^{-1} with a logarithmic stretch applied. (*e*) Core region in the F215N image, with features identified following RG; the contours are at 1, 2, 4, 10, 20, 40, and 100×10^{-15} ergs s^{-1} cm^{-2} Å^{-1}. (*f*) Composite three-color image of η Car: blue (F190N, 1.9 μm continuum), green (F187N + F216N, H I emission), and red (F212N + F215N, 2 μm continuum); each color has a logarithmic scale from zero to the peak intensity.

matching of the PSF; these artifacts were smoothed with a 1.5 pixel Gaussian. We show the resulting images for the F190N and F215N continuum filters in Figures 1*a* and 1*c* and the corresponding continuum-subtracted hydrogen Paα and Brγ images in Figures 1*b* and 1*d*. Some regions of the Brγ map are oversubtracted because of a small contribution from [Fe II] in the F215N continuum filter (see Allen et al. 1985); therefore, the Brγ fluxes given below are probably underestimated. The near-IR spectrum does not show any 2.122 μm H_2 emission (Allen et al. 1985), so the F212N filter was combined with the F215N filter to sample the ~2 μm continuum (*red*) in the composite-color image in Figure 1*f*. In Figure 1*f*, the red structures in and around the core show regions that suffer high extinction at $\lambda \lesssim 2$ μm. These structures are too cool for thermal dust emission to be important at ~2 μm (SGK).

The NICMOS observations were at a phase of ~0.14 in η Car's 5.5 yr spectroscopic cycle, near the start of the cycle when the high-excitation lines were beginning to recover from the spectroscopic event. The phase of the 1995 May ESO image in Figure 2*a* is ~0.53, roughly halfway through the cycle, when high-excitation lines are at their peak. The continuum-subtracted Brγ flux averaged over the filter bandwidth was 6.4×10^{-9} ergs s^{-1} cm^{-2} in 1995 and 2.3×10^{-9} ergs s^{-1} cm^{-2} in 1998. Thus, Brγ emission would contribute 2%–8% of the observed flux in a standard *K* filter ($\Delta\lambda = 0.4$ μm). The Paα flux integrated over the filter bandwidth was 1.7×10^{-8} ergs s^{-1} cm^{-2} in 1998. The Paα/Brγ ratio measured in the NICMOS data suggests that the southeast polar lobe causes an extinction of ~0.6 mag at $\lambda \sim 2$ μm (assuming case B recombination and an ionized gas temperature of 10^4 K in the core of the Homunculus).

3. DISCUSSION

3.1. *Observed Structure of the Homunculus*

The bipolar lobes show the same general morphology in NICMOS images as is observed in the near-IR/optical (SGK; Morse et al. 1998), and the mottled appearance of the lobes in optical *HST* images is repeated in the NICMOS images (Figs. 2*e* and 2*f*). Dark regions in optical images, such as the dust lanes and the prominent spot in the middle of the southeast polar lobe, correspond to dark regions in the near-IR as well. This argues that the dark features are regions of relatively low dust density, which correspond to a paucity of scattered light, rather than regions of high extinction. Forward scattering may cause the features on the near side of the lobe to appear much brighter than those on the far side.

The new near-IR images confirm the structure in the equatorial ejecta observed by SGK, although the higher resolution attained with NICMOS shows their clumpy structure in greater detail. The near-IR equatorial ejecta show several knots that are brighter relative to the polar lobes than at optical wavelengths. These are not necessarily coincident with the brightest optical structures, such as the "fan" (Fig. 1*e*). The relationship between the optical and IR structures in the equatorial ejecta was described in detail by Smith, Gehrz, & Krautter (1999). It is not clear how the outer equatorial structures relate to the equatorial structures in the core of the Homunculus.

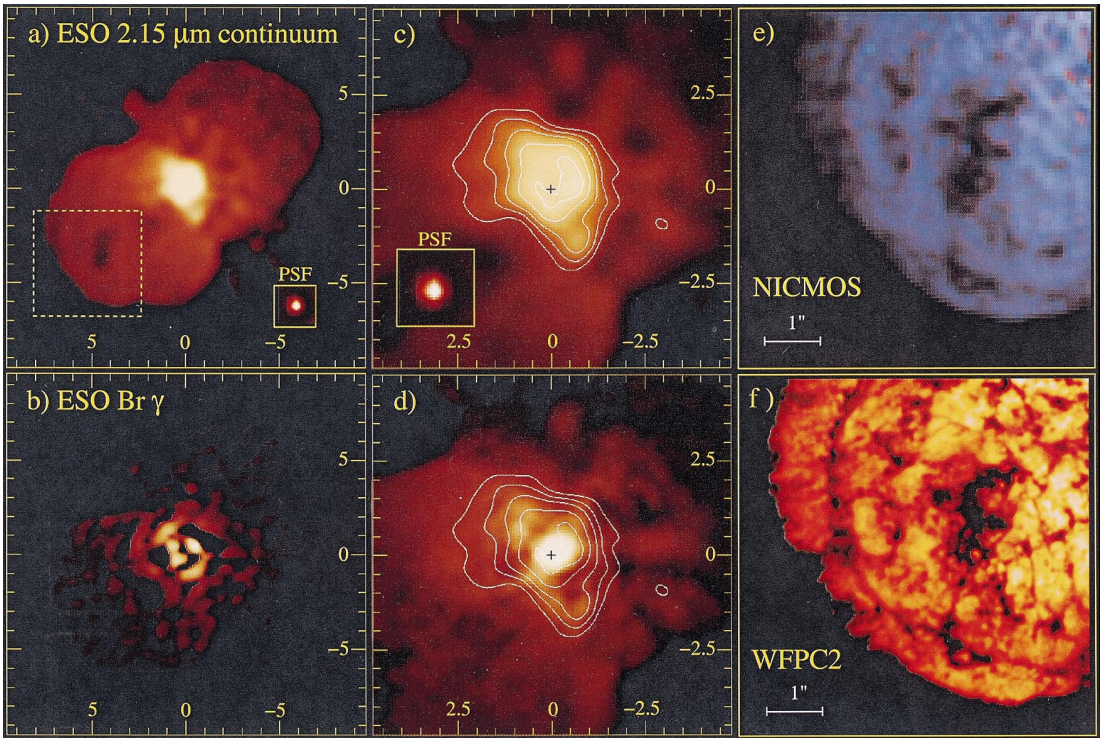

FIG. 2.—(*a*) 1995 ESO 2.15 μm continuum image. The image of a field star with FWHM ≈ 0″.4 is shown in the lower right-hand corner. (*b*) 1995 ESO continuum-subtracted Brγ emission. (*c*) The core region of (*a*) with the same contour levels as in Fig. 1*e* [the point source from (*a*) is shown in lower left-hand corner on the same expanded scale]. (*d*) The core region of 1998 NICMOS F215N image with 1995 ESO contours superposed. (*e*) Detail of the southeast polar lobe in the NICMOS images with the same color scheme as Fig. 1*f*. (*f*) Detail of the southeast polar lobe in an optical *HST* image. The dotted box in (*a*) shows the region included in (*e*, *f*).

3.2. *The Inner Core*

The NICMOS images reveal structures in the bright core of the nebula that differ from those seen at optical wavelengths. These are discussed below and labeled in Figure 1*e*, where we have adopted RG's terminology.

An elongated emission feature that wraps around the central object is seen in both the NICMOS and ground-based images, but is more prominent in the former because the central object is more compact at certain epochs, as discussed below. Assuming that this structure corresponds to an equatorial torus (Fig. 1*c*), it is evident that the torus does not have an azimuthally symmetric brightness distribution. The emission is clumpy, with most of the emission coming from the far side of the torus. There is considerable reddening of the torus, as evidenced by Figure 1*f*. Assuming that the torus is circular, its inclination angle is $i \approx 64°$ (where $i = 90°$ is edge-on; RG measure $i = 63° \pm 5°$), and the position angle of the rotational axis is P.A. = 120° ± 2°. A straightforward physical interpretation of the torus is that it represents a lumpy equatorial ring of dust and gas at distances of a few 10^3 AU from the central star. The near-IR light from the torus is probably produced primarily by a combination of scattered light from the central object and intrinsic line emission (see Figs. 1*b*, 1*d*, and 2*b* and SGK). An elongated multiple-peaked structure is also observed in the mid-IR, and the condensations are observed to shift farther from the star with increasing wavelength (Hackwell et al. 1986; SGK). The near-IR torus and mid-IR condensations may be contiguous structures in the equatorial plane, with different IR wavelengths tracing a range of dust temperatures and scattering optical depths. It seems probable that the near- and mid-IR emission described above traces a flattened distribution of dust grains that have formed in a high-density equatorial post-eruption stellar wind. The presence of a similar extended equatorial disk was inferred from optical speckle-masking imaging polarimetry observations (Falcke et al. 1996).

In the NICMOS images, the bright central object is elongated along the major axis of the Homunculus, and the extended emission within 0″.5 can be attributed to the southeast condensation discovered by RG and to a northwest condensation that is not as well separated from the central point source (Fig. 1*e*). In the near-IR continuum and line images, the southeast condensation is smaller and fainter than the northwest condensation, and the northwest condensation appears to have a relatively wide opening angle of ∼50° relative to the central star. RG also identified a "jet" extending beyond the southeast condensation, and a polar jet at this location was inferred from Hα polarization data (Falcke et al. 1996). This feature is seen in the NICMOS images but not in the ESO image (compare Figs. 2*c* and 2*d*); perhaps this jet is periodically illuminated during the 5 yr spectroscopic cycle.

The southeast and northwest condensations are clearly detected in the 1995 ESO continuum image (Fig. 2*c*), but the overall morphology of the bright inner core is very different from that seen in the 1998 NICMOS images. In particular, the bright central point source seen at the position of the central star in the NICMOS images appears more extended and shell-like in 1995. The cross in Figure 2*c* marks the position of the central star as measured in an optical 1995 *HST* image, which was aligned using two stars in the field to the northeast of the Homunculus. The larger size and shell structure of the bright inner core in the 1995 ESO image is not an artifact of the deconvolution. It shows a similar structure (although less well

defined) before deconvolution, and stars included in the field of view of the 1995 image (see SGK) are pointlike with a FWHM of 0″.4. This is much smaller than the size of the shell structure in η Car, which is ∼1″.5. Thus, we conclude that the bright central core surrounding the star has changed its observed morphology dramatically between 1995 and 1998, appearing more pointlike in 1998.

Indirect confirmation of this scenario comes from an examination of the near-IR images presented by RG. Their 1991 April (phase = 0.79) images show a pointlike central source at *JKL′M* within 1.5 yr of the spectroscopic event at 1992.5. However, their 1994 April (phase = 0.33) *K* image, obtained roughly 1 yr before SGK's 1995 images, has low-level contours revealing a shell-like structure similar to that seen in the 1995 images (Fig. 2*c*). In the 1994 April *K* image, the brightest source is located on the southwest edge of this "shell" and is seen at a higher contrast with respect to the surrounding nebulosity than in 1995.

To what can we attribute the morphological changes of the inner core? Whitelock et al. (1983) have studied the near-IR photometric variability of η Car and concluded that it would be important to determine if the photometric variations are accompanied by changes in the observed morphology of the nebulosity. Our comparison of the 1995 and 1998 near-IR images would suggest that they are. These morphological changes might be related to three types of variability that have now been documented for η Car: (1) the secular increase in brightness of $\lesssim$0.03 mag yr^{-1} at *K* (Whitelock et al. 1994), (2) a recently discovered outburst in which the central star has doubled its brightness at optical wavelengths (Davidson et al. 1999), and (3) the ∼5 yr period (Whitelock et al. 1994; Daminelli 1996). The 2.15 μm flux in a 1″ aperture increased by a factor of ∼2 from 8.8×10^{-12} ergs s^{-1} cm^{-2} Å^{-1} in 1995 to 1.7×10^{-11} ergs s^{-1} cm^{-2} Å^{-1} in 1998. During the same time period, the 2.15 μm flux from the entire Homunculus increased by 13%: $(2.08–2.43) \times 10^{-11}$ ergs s^{-1} cm^{-2} Å^{-1}. Thus, changes in spatial morphology related to variability of types 1 or 2 are implicated. However, variability of type 3 is implicated by the continuum-subtracted Brγ emission, which was a factor of 2.8 stronger in 1995 than in 1998. This is remarkably similar to the 1995/1998 3 cm continuum flux ratio of ∼2.5 (estimated from Fig. 3 in Duncan et al. 1999); the 3 cm flux varies conspicuously during η Car's spectroscopic cycle. Morphological changes may also be related to the ∼5 yr period. For example, all near-IR images during 1991–1998 are consistent with the interpretation that a central source that is pointlike within a year of the spectroscopic event is transformed to an extended shell source in between spectroscopic events. This resembles changes in the radio continuum morphology of η Car during the spectroscopic cycle (Duncan, White, & Lim 1997; Duncan et al. 1999), which show that following a spectroscopic event, a radio continuum point source expands to a bipolar or shell-like structure. The shell structure becomes more distorted as the 5 yr cycle proceeds and then returns to a point-source configuration during the next spectroscopic event. In fact, the morphology of the bright core in the 1995 ESO image is almost identical to that in the 1995 December radio image presented by Duncan et al. (1997), although there is a slight discrepancy as to the position of the central star. In the model proposed by Duncan et al., the observed changes are not due to expanding gas structures but to ionization of previously deposited gas at increasing distances from the star. Indeed, the IR structures that expand to projected distances of ∼1″ from the star during half of the 5 yr spectroscopic cycle would implicate velocities of at least 4000 km s^{-1}. This is much larger than any velocities directly observed in the core region of the Homunculus. The similarity in the morphological changes observed in the radio and the IR suggests that the near-IR morphological changes in the central core of η Car are due either to near-IR free-free or recombination line emission from ionized circumstellar gas or to thermal emission from very hot dust grains that are heated by collisions with the ionized gas (or all of these). If the emission in the southeast and northwest condensations is thermal emission from hot dust, the grains must be significantly hotter than their blackbody temperatures of ∼400 K for projected distances of ∼1000 AU from the star in order to emit significantly at 2 μm. This would require the grains to be very small iron or graphite grains with significant superheat.

The observed morphological changes indirectly argue that the pointlike emission observed in the near-IR soon after the spectroscopic event is not emission from the star's photosphere or wind but instead comes from variably illuminated circumstellar ejecta. This conjecture—that the majority of the near-IR radiation does not come directly from the star itself—has important ramifications for binary models that rely on near-IR emission lines. It will be important to monitor η Car throughout the ∼5 yr cycle to confirm that the observed changes are indeed *periodic*. However, the picture may now be complicated by the star's recent outburst, which is apparently not related to the spectroscopic cycle (Davidson et al. 1999).

We have benefited from numerous discussions about η Car with K. Davidson and R. Humphreys. Optical *HST* images prepared by J. Morse have been valuable for comparison with the IR images.

REFERENCES

Allen, D. A., Jones, T. J., & Hyland, A. R. 1985, ApJ, 291, 280
Daminelli, A. 1996, ApJ, 460, L49
Davidson, K. 1971, MNRAS, 154, 415
Davidson, K. et al. 1999, AJ, 118, 1777
Duncan, R. A., White, S. M., & Lim, J. 1997, MNRAS, 290, 680
Duncan, R. A., White, S. M., Reynolds, J. E., & Lim, J. 1999, in ASP Conf. Ser. 179, Eta Carinae at the Millennium, ed. J. A. Morse, R. M. Humphreys, & A. Daminelli (San Francisco: ASP), 54
Falcke, H., Davidson, K., Hofmann, K. H., & Weigelt, G. 1996, A&A, 306, L17
Hackwell, J. A., Gehrz, R. D., & Grasdalen, G. L. 1986, ApJ, 311, 380
Hyland, A. R., et al. 1979, ApJ, 233, 145
Meaburn, J. 1999, in ASP Conf. Ser. 179, Eta Carinae at the Millennium, ed. J. A. Morse, R. M. Humphreys, & A. Daminelli (San Francisco: ASP), 89
Mitchell, R. M., Robinson, G., Hyland, A. R., & Jones, T. J. 1983, ApJ, 271, 133
Morse, J. A., et al. 1998, AJ, 116, 2443
Morse, J. A., Humphreys, R. M., & Daminelli, A., eds. 1999, ASP Conf. Ser. 179, Eta Carinae at the Millennium (San Francisco: ASP)
Rigaut, F., & Gehring, G. 1995, in Rev. Mexicana Astron. Astrofis. Ser. Conf. 2, The η Carinae Region: A Laboratory of Stellar Evolution, ed. V. Niemela, N. Morrell, & A. Feinstein (Mexico, DF: Inst. Astron., UNAM), 27 (RG)
Smith, C. H., et al. 1995, MNRAS, 273, 354
Smith, N., Gehrz, R. D., & Krautter, J. 1998, AJ, 116, 1332 (SGK)
———. 1999, in ASP Conf. Ser. 179, Eta Carinae at the Millennium, ed. J. A. Morse, R. M. Humphreys, & A. Daminelli (San Francisco: ASP), 31
Whitelock, P. A., et al. 1983, MNRAS, 203, 385
———. 1994, MNRAS, 270, 364